THE JOURNAL OF PHYSICAL CHEMISTRY C

Article

pubs.acs.org/JPCC

Sticking with the Pointy End? Molecular Configuration of Chloro Boron-Subphthalocyanine on Cu(111)

Nahid Ilyas,[†,#] Shashank S. Harivyasi,[‡,#] Percy Zahl,[§] Rocio Cortes,[§] Oliver T. Hofmann,[‡] Peter Sutter,[§,∥] Egbert Zojer,[*,‡] and Oliver L. A. Monti[*,†,⊥]

[†]Department of Chemistry and Biochemistry, University of Arizona, Tucson, 1306 E. University Boulevard, Tucson, Arizona 85721, United States

[‡]Institute of Solid State Physics, NAWI Graz, Graz University of Technology, Petersgasse 16, 8010 Graz, Austria

[§]Center for Functional Nanomaterials, Brookhaven National Laboratory, Upton, New York 11973, United States

[∥]Department of Electrical and Computer Engineering, University of Nebraska-Lincoln, Lincoln, Nebraska 68588, United States

[⊥]Department of Physics, University of Arizona, Tucson, 1118 E 4th Street, Tucson, Arizona 85721, United States

Supporting Information

ABSTRACT: In this combined low-temperature scanning tunneling microscopy (STM) and density functional theory (DFT) study, we investigate self-assembly of the dipolar nonplanar organic semiconductor chloro boron-subphthalocyanine (ClB-SubPc) on Cu(111). We observe multiple distinct adsorption configurations and demonstrate that these can only be understood by taking surface-catalyzed dechlorination into account. A detailed investigation of possible adsorption configurations and the comparison of experimental and computational STM images demonstrates that the configurations correspond to "Cl-up" molecules with the B−Cl moiety pointing toward the vacuum side of the interface, and dechlorinated molecules. In contrast to the standard interpretation of adsorption of nonplanar molecules in the phthalocyanine family, we find no evidence for "Cl-down" molecules where the B−Cl moiety would be pointing toward the Cu surface. We show computationally that such a configuration is unstable and thus is highly unlikely to occur for ClB-SubPc on Cu(111). Using these assignments, we discuss the different self-assembly motifs in the submonolayer coverage regime. The combination of DFT and STM is essential to gain a full atomistic understanding of the surface−molecule interactions, and our findings imply that phthalocyanines may undergo surface-catalyzed reactions hitherto not considered. Our results also indicate that care has to be taken when analyzing possible adsorption configurations of polar members of the phthalocyanine family, especially when they are adsorbed on comparably reactive surfaces like Cu(111).

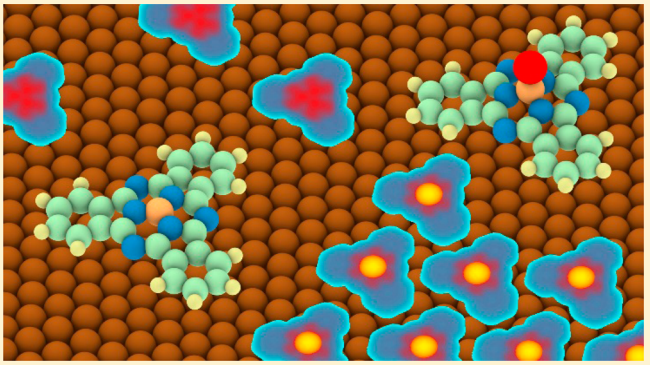

1. INTRODUCTION

Well-defined structure−function relationships relating molecular structure to thin film structure and ultimately interfacial energy level alignment have been difficult to establish for many organic semiconductor/metal surface combinations due to the high structural diversity of the organic molecules of interest.[1−7] This is further compounded by frequent polymorphism and often complex phase diagrams for organic thin film growth.[8−10] The root cause lies likely in the fact that the important interactions, ranging from dipole repulsion and van der Waals interactions to charge-transfer related forces, occur on comparable energy scales. This makes predictive insight into the molecular adsorption and resulting thin film structure for arbitrary organic semiconductors still challenging.[11−13]

Nonplanar members of the phthalocyanine family provide a step toward addressing such issues. Their shuttle-cock shape results in a limited number of different adsorption configurations that have been widely interpreted as stemming from the polar axial group either facing vacuum ("up") or the supporting surface ("down").[11,13−22] In principle, this offers an attractive opportunity for investigating the consequences of different adsorption configurations and surface-molecule coupling on energy level alignment and thin film structure for the same molecule.

The present paper reports on the detailed investigation of chloro boron-subphthalocyanine (ClB-SubPc, Figure 1) on Cu(111). ClB-SubPc is an important member of the class of three-fold symmetric SubPc molecules, which displays distinctly different structures upon adsorption on (111) coinage metal surfaces.[23−27] On Cu(111), scanning tunneling microscopy

Received: December 2, 2015
Revised: March 10, 2016
Published: March 10, 2016

DOI: 10.1021/acs.jpcc.5b11799
J. Phys. Chem. C 2016, 120, 7113−7121

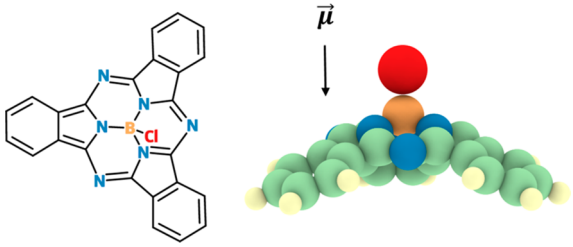

Figure 1. (a) Chemical structure and (b) shuttle-cock shaped geometry of a gas-phase ClB-SubPc molecule. The permanent dipole moment is also indicated. Color code of atoms: Cl, red; C, pale green; N, blue; B, orange; H, pale yellow.

(STM) reveals two adsorption configurations,[26,27] while on both Ag(111) and Au(111) only a single adsorption configuration for all ClB-SubPc molecules was found.[23−25] Still, the nature of the different adsorbate configurations and their consequences for self-assembly are not yet fully understood.

Here, we combine findings from low-temperature scanning tunneling microscopy (LT-STM) and dispersion-corrected density functional theory (DFT) to elucidate in detail the adsorption of ClB-SubPc on Cu(111) and its consequences for self-assembly in the submonolayer regime. We provide for the first time both experimental and theoretical evidence that the different adsorbate configurations on Cu(111) are in fact two distinct molecules, (i) intact ClB-SubPc and (ii) B-SubPc, the result of a surface-catalyzed dechlorination reaction. Our findings may apply more broadly to dipolar phthalocyanines on metal surfaces and highlight that surface-catalyzed reactions must be taken carefully into account when investigating such interfaces.

2. MATERIALS AND METHODS

2.1. Scanning Tunneling Microscopy. Cu(111) was cleaned by repeated cycles of Ar^+ sputtering (1.0 kV) and annealing at 830 K. ClB-SubPc was purchased from Sigma-Aldrich (85%) and was further purified by a single cycle of gradient sublimation in a custom-built furnace, where it formed large (≥1 cm) crystal sheets of high purity. Prior to deposition, the purified ClB-SubPc was degassed overnight in a home-built water-cooled Knudsen cell under ultrahigh vacuum (UHV) conditions (<2 × 10^{-9} Torr) slightly below its sublimation point at 433 K. The molecular film thickness on the substrate was monitored by a quartz crystal microbalance and calibrated against a statistical ensemble of STM images. The molecules were deposited at a slow rate corresponding to an average growth rate of one monolayer equivalent (MLE) in ∼28 min. Here, a full MLE refers to a hypothetical layer formed with molecules in a high-density hexagonal-closed packing arrangement (see Section 3.2 for more detail). Following deposition at temperatures variously chosen between 150 and 225 K, the surface was quenched to 77 K and the sample was transferred immediately (<5 min) to a cryogenic UHV scanning tunneling microscope (LT-STM) held at 5 K and equipped with GXSM custom control.[28,29] All images were acquired with electrochemically etched tungsten tips in constant-current mode and were subsequently further processed using the WSxM software package.[30]

2.2. Computational. All calculations of the ClB-SubPc/Cu(111) interface were carried out using the Fritz Haber ab initio molecular simulations package (FHI-aims)[31] with "tight" settings, as shipped with the code, and employing the dispersion corrected PBE+vdW^{surf} functional.[32−34] The functional provides remarkable reliability for both the geometric[35] and electronic structure[36] of metal−organic interfaces. The repeated-slab approach was employed in an orthogonal ($7 \times 4\sqrt{3}$) unit cell with periodic replicas of the metal slab/adsorbate separated by at least 25 Å of vacuum. Each unit cell contained one molecule of ClB-SubPc (corresponding to a coverage of 0.54 MLE). This results in a distance of at least 5.14 Å between each molecule and its periodic image. The registry of the molecule with the Cu(111) surface and its orientation relative to the high-symmetry directions of the surface were deliberately varied prior to geometry optimization in order to scan multiple local minimum geometries (vide infra). The metal substrate in the unit cell was represented by six layers of Cu exposing the (111) surface. The bottom four layers were frozen at the bulk positions during geometry optimization. Dispersion correction for the Cu−Cu atom pairs of the substrate was disabled. The replicas were electrostatically decoupled using a self-consistently determined discontinuity of the electrostatic energy in the vacuum region.[37] A 2 × 2 × 1 Monkhorst−Pack[38] k-point grid was used. The convergence criterion for the energy self-consistency cycle was 10^{-6} eV and the geometry was relaxed until the maximum residual force component per atom was below 0.01 eV/Å.

The adsorption energy, E_{ads}, for all cases was calculated as

$$E_{ads} = E_{inter} - (E_{Cu} + E_{ML})$$

where E_{inter} refers to the energy of the interacting ClB-SubPc/Cu(111) system; E_{Cu} is the energy of a pristine Cu(111) slab with the top two layers relaxed, and E_{ML} is the energy of relaxed free-standing monolayer of ClB-SubPc molecules. Simulated STM images were obtained using the Tersoff−Hamann approximation[39] at a sample bias of −2 V and with an active tip radius of 1.5 Å, following the procedure described in ref 40. All images showing 3D structures have been created using OVITO.[41]

3. RESULTS AND DISCUSSION

3.1. Overview. In order to investigate the molecular self-assembly of ClB-SubPc on Cu(111), we prepared thin films in a wide range of conditions, varying surface coverage in particular. For all coverages and growth conditions, we find exclusively two markedly different STM contrasts for the molecular adsorbate in the first layer, as shown in a representative close-up constant-current STM image in Figure 2a. They are labeled

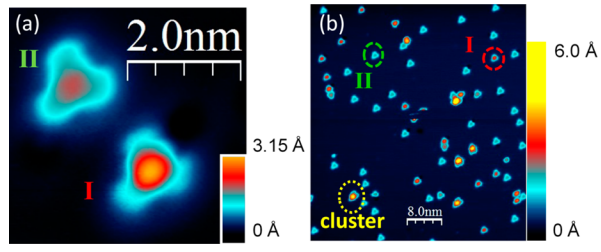

Figure 2. Representative STM images showing two adsorbate species, classified as type **I** (high) and type **II** (low) depending on the conductance in the molecular center. (a) Close-up (V_S = 0.5 V; I_t = 150 pA; T = 5 K). (b) Overview (0.04 MLE coverage; V_S = −1.94 V; I_t = 50 pA; T = 5 K). Films grown at 205 K. An example of a "cluster" feature is also marked.

DOI: 10.1021/acs.jpcc.5b11799
J. Phys. Chem. C 2016, 120, 7113−7121

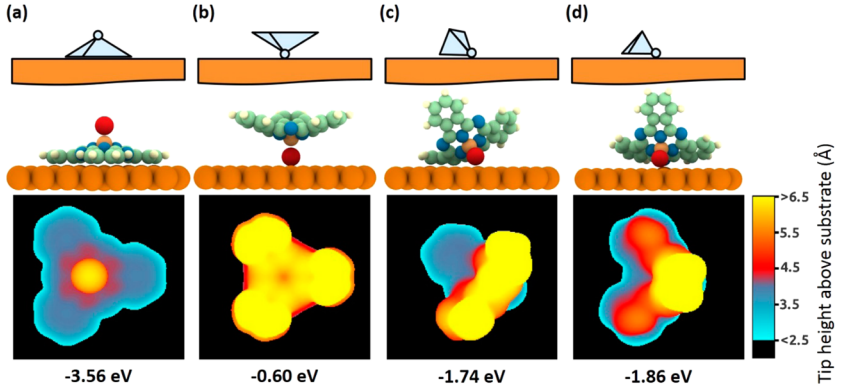

Figure 3. Adsorption configurations investigated by DFT: (a) Cl-up, (b) Cl-down, and "fallen" with (c) one or (d) two isoindole unit(s) in contact with the Cu(111) substrate. Top row: Schematic. Second row: Atomistic picture based on DFT. Third row: Corresponding simulated STM image (V_S = −2 V). Bottom row: Calculated adsorption energy for the configuration. Color code of atoms: Cl, red; C, pale green; N, blue; B, orange; H, pale yellow.

I and **II** and are characteristic of the two STM contrasts obtained throughout all images. The overview at low coverage in Figure 2b indicates that type **I** and **II** molecules are the only species on the surface other than occasional small aggregates (labeled "cluster" in Figure 2b) whose structure is not resolved. The contrast of the type **I** and **II** molecular adsorbates is remarkably independent of the tip−surface voltage (reported here as sample bias V_S) at least over the investigated window from −2.5 V to +0.5 V. The salient difference between the two molecular types is that molecules of type **I** exhibit a bright center while for type **II** the conductance increase in the molecular center is much less pronounced. Similar observations have been reported for various dipolar metal phthalocyanines on a range of different surfaces.[13,17−19,22] The two distinct contrasts in STM images of dipolar phthalocyanines are usually interpreted as originating from two molecular adsorption configurations that differ primarily in the spatial orientation of the axial ligand, either protruding into the vacuum side of the interface (**I**) or facing the surface (**II**). The microscopic detail of how the axial ClB ligand in type **II** faces the Cu(111) surface is however rather unclear. This is important, because the two configurations of ClB-SubPc on Cu(111) exhibit fundamentally different thin film formation propensities as shown below. The differences in the self-assembly behavior suggest that the surface−molecule interactions differ substantially for the two configurations.

To investigate this issue in more detail, we used quantum-mechanical simulations to consider a broad range of possible adsorption configurations. These configurations are shown in Figure 3 in schematic and atomistic pictures where the latter are the result of DFT-based geometry optimizations.

First, we simulated the two most widely proposed configurations for similar systems: Molecules with chlorine atoms protruding toward vacuum (conventionally called the "Cl-up" system, Figure 3a), and molecules with chlorine atoms oriented toward the substrate (usually referred to as "Cl-down", Figure 3b). Out of all possibilities considered, the Cl-up configuration results in the most stable adsorbate geometry, with an adsorption energy of −3.56 eV and a simulated STM image that is remarkably similar to those observed for type **I** molecules. Our simulations reveal however that the proposed Cl-down configuration does not form readily on this surface; it can only be obtained whether the molecular C_{3v}-symmetry axis is aligned exactly perpendicular to the substrate. It is also accompanied by a comparatively small adsorption energy of only −0.60 eV. This surface-molecule geometry is thermodynamically not stable toward the formation of one of two possible "fallen" configurations, which have either a single isoindole (Figure 3c) or two isoindole groups in contact with the substrate (Figure 3d). Though not as strongly adsorbed as Cl-up, both "fallen" configurations are significantly more stable than the upright-standing Cl-down structure. Most strikingly, the simulated STM images in Figure 3 for Cl-down and "fallen" look profoundly different from either the type **I** or the type **II** molecules observed in the experimental images. Note that the brightest features in Figure 2b, labeled "Cluster", have too large of an apparent height to be consistent with the "fallen" configurations. This suggests a different nature of the type **II** configuration. To clarify this finding, we investigate in the following sections each of the two adsorption types in more detail relating the atomistic structure of the adsorbate geometry to (sub)monolayer growth. We then explore the possibility of a surface-catalyzed chemical modification of the ClB-SubPc molecules as the origin for configuration **II**.

3.2. Origin of Adsorbate Type I: Cl-up. Among the four simulated configurations (Figure 3), the Cl-up system reproduces all the salient characteristics of adsorbate type **I** satisfactorily. Thus, the results of the corresponding calculations can be used to better understand the atomistic properties of the adsorbate: In the simulated Cl-up configuration, the molecule flattens considerably upon surface adsorption. When measuring the molecular height, defined as the distance between the Cl atom and the plane spanned by the six outermost C atoms (see Figure S1 in SUI), one observes a decrease from 4.46 Å (gas phase) to 3.25 Å (adsorbed). During adsorption, the B−Cl bond length remains virtually unchanged at 1.86 Å, as the flattening almost exclusively affects the π-backbone of the molecule. Consequently, the Cl atom protrudes sharply from the backbone and results in a large contrast enhancement at the center of the molecule in the simulated STM image. This is indeed also the case for the measured images of the Cl-up system (Figure 2).

3.3. Growth of Adsorbate Type I: Cl-up. Beyond the very lowest coverages investigated, we observe a small number of disordered molecular clusters and bilayer structures (Figure 4, marked by green circles and discussed in more detail in Section 3.5) and the nucleation of ordered islands. For type **I** molecules, self-assembly manifests itself in the coexistence of

DOI: 10.1021/acs.jpcc.5b11799
J. Phys. Chem. C 2016, 120, 7113−7121

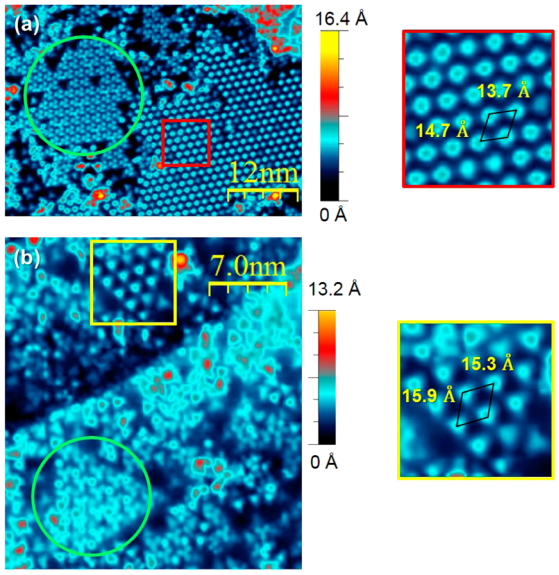

Figure 4. STM images of 0.50 MLE ClB-SubPc on Cu(111) prepared at 205 K showing the coexistence of different types of ordered islands. (a) Two-dimensional hcp islands of Cl-up molecules with detail and unit cell dimensions (close-up red box in right panel). Imaging conditions: $V_S = -2.5$ V; $I_t = 50$ pA, 5 K. (b) Low-density hcp Cl-up islands with close-up detail and unit cell dimensions in right panel. Imaging conditions: $V_S = -2.0$ V; $I_t = 50$ pA, 5 K. Note that the height scale bar in both panels is different from the ones used in Figure 2 in order to accommodate the much wider range of heights in this image caused by step edges, terraces, and bilayer structures. Also, the contrast between panels (a) and (b) differs due to the presence of a step in (b). Green circles: bilayer structures, discussed in detail in Section 3.5. Red and yellow squares: close-up of the two observed hcp structures.

two kinds of ordered islands with different packing densities, interspersed with randomly distributed isolated molecules. Most notable at this and similar coverages is the formation of large hexagonally close-packed (hcp) islands (Figure 4a and red square close-up) that consist predominantly of Cl-up (type **I** molecule). These islands are densely packed with measured unit cell dimensions of 13.7(10) Å × 14.7(10) Å, an acute angle of 60°, and an area of 174 Å^2 (see Figure S2 in SUI for a molecular model). Similar hcp structures have also been reported for ClB-SubPc islands on Ag(111) and Au(111) surfaces,[23,24] albeit for the suggested Cl-down adsorbate configuration. On Cu(111), after annealing to 350 K, a (9 × 9) honeycomb structure was reported instead.[27] We used these islands to define coverage in terms of MLE (cf. Section 2). Less frequent are low-density hcp islands (Figure 4b and yellow square close-up), which also consist predominantly of adsorbates of type **I** (Cl-up). The unit cell dimensions for these islands are 15.9(10) Å × 15.3(10) Å, and the acute angle of the unit cell is again ∼60°, resulting in a unit cell area of 220 Å^2. This structure has not been previously reported. Although unit cell measurements are uncertain to within approximately 1 Å due to piezo hysteresis, low- and high-density hcp structures are clearly distinct and correspond to different molecular growth on the Cu(111) surface. The slightly different shape of the molecules in these two island kinds is likely due to finite STM tip-size effects, slightly different local DOS, and the *z*-dependence of the tunneling matrix element.

Close inspection of these islands shows that most molecules are oriented along the same surface direction although one might conclude that the six-fold symmetry of the top-layer of the surface together with the three-fold molecular symmetry should allow for two molecular orientations on the surface. Contrary to this, molecules rotated by 60° are found primarily at the edges of hcp islands (vide infra).

A computational survey of different surface-molecule registries, summarized in Figure 5, shows that the most favorable adsorption geometry places the axial ClB ligand above one of the two hollow sites (hcp and face-centered cubic (fcc) hollow).

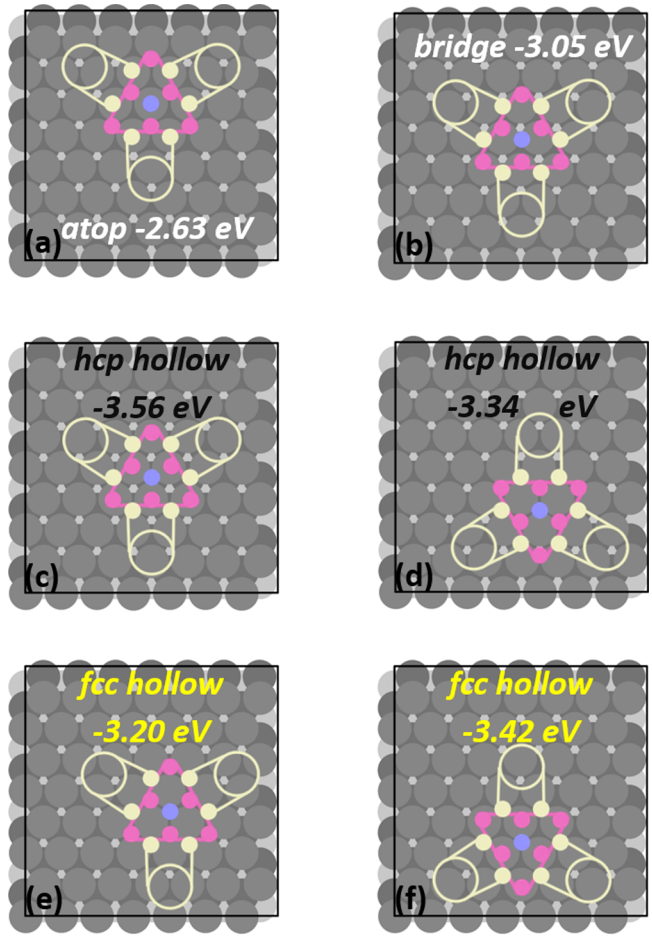

Figure 5. ClB-SubPc Cl-up on (a) atop site, (b) bridge site, (c) hcp hollow site with maximum N−Cu registry (referenced as 0°), (d) hcp hollow site with reduced registry (rotated by 60°), (e) fcc hollow site with reduced registry (0°), (f) fcc hollow site with maximum registry (rotated by 60°). Numbers in all schematics represent calculated adsorption energies. The top three layers of the copper slab are color coded in gray (top layer), dark gray (second layer) and light gray (third layer) respectively. N atoms are shown in purple, the C frame is beige, and the B−Cl moiety is blue.

Atop (Figure 5a) and bridge (Figure 5b) sites are significantly less stable, and adsorption at hollow sites is thermodynamically preferred. The DFT simulations predict that the energy difference between different rotational orientations for molecules adsorbed at either hcp or fcc hollow site is at least 0.2 eV. Consequently, at those sites orientations with near-perfect registry between the isoindole N atoms and the Cu atoms in the top layer of the (111) surface are expected (Figure 5c,f). Strong Cu−N interactions have been reported to be favorable also, for example, for azobenzene on Cu(111).[42] This alone would still allow for two orientations of the

DOI: 10.1021/acs.jpcc.5b11799
J. Phys. Chem. C 2016, 120, 7113−7121

molecular adsorbates on the surface, but the calculations predict that a location of the B atom at the hcp-hollow site is energetically preferable by ∼0.14 eV over the fcc-hollow site, hinting toward an interaction of the molecule also with the second layer of the substrate. Consequently, it is not sufficient to consider only the topmost substrate layer and the actual three-fold rotational symmetry of the substrate is crucial for explaining why only one orientation of the molecules is observed experimentally on the Cu(111) surface. This is in spite of the fact that calculated energy differences for different orientations are small compared to the total adsorption energy of −3.6 eV and potentially approach the limit of accuracy of the applied computational methodology. Experimentally, a definitive identification of surface registry has not been possible; however, a correlation of the isolated Cl-up molecule with an atomically resolved Cu(111) lattice is in tentative agreement with adsorption at a hollow site (see SUI Figure 3). Defects in the sense of molecules rotated by 60° occur principally at boundaries of well-ordered islands (vide infra).

3.4. Origin of Adsorbate Type II: Dechlorination. The identification of the nature of the adsorbate type **II** turns out to be considerably more complex than for type **I**. As discussed above, "fallen" geometries would result in a symmetry reduction in the STM pictures, which is not observed experimentally. Thus, the fallen configurations can be immediately excluded as possible candidates for the adsorbate type **II**.

The upright Cl-down configuration with the ClB-SubPc molecule precariously balanced along its B−Cl bond axis indeed yields simulated STM images preserving the molecular C_{3v} symmetry (Figure 3b). However, contrary to the experimental STM images of type **II** molecules, in the simulated image the conductance is highest in the isoindole groups of the heterocycle with a contrast depression in the molecular center. Moreover, for such a configuration the apparent height of the isoindole groups is larger than even that of the Cl atom in Cl-up molecules, again at variance with the experimental observations. The fact that this is not a configuration likely found on the Cu(111) surface is further emphasized by the rather low adsorption energy of −0.60 eV, dramatically smaller than all other adsorption configurations investigated thus far (vide supra). Additionally, such a configuration would likely entail a rather low rotational barrier around the C_3 axis bearing in mind the significant distance between the molecular backbone and the metal surface. Consequently, rotational motion is not expected to be frozen even at 5 K, resulting in random orientations of type **II** molecules and rotational blurring. Yet, none of the experimentally obtained STM images show any indication of rotational motion, and all type **II** ClB-SubPc molecules appear identically oriented on the Cu(111) surface. To summarize, by comparing atomistic simulations with experiments we find no stable Cl-down configuration that preserves the experimentally observed three-fold molecular symmetry while simultaneously leaving the B−Cl bond intact.

In light of these findings, we next consider surface-catalyzed dechlorination of ClB-SubPc. To this end, we removed the chlorine atom from the molecule in the fallen configuration with one isoindole group in contact with the substrate and proceeded to relax the resulting dechlorinated structure. Because of the sizable adsorption energy of Cl atoms on Cu(111),[43] the Cl atom is expected to remain on the substrate. In order to minimize residual interactions between the molecular fragment and the Cl atom, the Cl atom was moved in our calculations 6 Å away from the dechlorinated molecule (Figure 6). Consistent with the observations of dechlorination

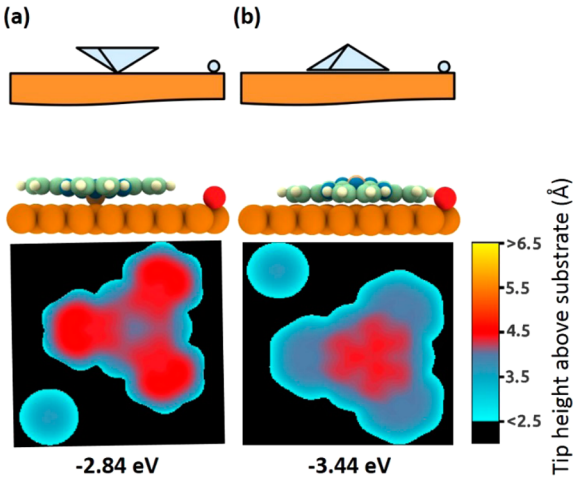

Figure 6. Dechlorinated configurations investigated by DFT: (a) DeCl-down and (b) DeCl-up. Top row: Schematic. Second row: Atomistic Picture. Third row: Simulated STM images (V_S = −2 V). Bottom row: Calculated adsorption energies for each configuration. Color code of atoms: Cl, red; C, pale green; N, blue; B, orange; H, pale yellow.

for porphyrin derivatives,[44,45] we investigated two likely configurations, referred to in the following as "DeCl-down" (with the Cl atom below the molecular backbone, cf. Figure 6a) and "DeCl-up" (with the Cl atom above the molecular backbone, cf. Figure 6b). Our calculations suggest that the DeCl-up configuration is considerably more stable than DeCl-down; the transition from DeCl-down to DeCl-up is thermodynamically favored by 0.6 eV (see Figure S4 in SUI for further discussion), and the net adsorption energy for the dechlorinated DeCl-up molecule plus a chlorine adatom is −3.44 eV. Remarkably, other than the Cl-up configuration this is the most stable configuration we were able to identify. It is also more favorable by 1.58 eV than the fallen configuration (with two isoindole in contact with the substrate), which is the energetically closest configuration that preserves the molecule's chemical structure and has the molecule's Cl atom oriented toward the surface. On the basis of these thermodynamic considerations summarized in Table 1, we associate type **II** molecules observed experimentally in the adsorption of ClB-SubPc on Cu(111) with the DeCl-up configuration.

This association is further reinforced when comparing the simulated STM images for the two DeCl possibilities with experimental STM images. Simulated DeCl-up shows a

Table 1. Adsorption Energy for all Considered Configurations of (Cl)B-SubPc molecule on Cu(111)[a]

configuration	adsorption energy (eV)
Cl-up	−3.56
Cl-down	−0.60
fallen; one isoindole in contact with substrate	−1.74
fallen; two isoindole in contact with substrate	−1.86
DeCl-up	−3.44
DeCl-down	−2.84

[a]See text for detailed explanation of all configurations which are also visualized in Figures 3 and 6.

DOI: 10.1021/acs.jpcc.5b11799
J. Phys. Chem. C 2016, 120, 7113−7121

moderate apparent height increase in the center of the molecule (Figure 6b), which agrees well with the experimentally determined constant current images for adsorbate type **II** (Figure 2). In contrast, simulated DeCl-down exhibits a contrast depression in the molecular center (Figure 6a) at variance with experiments. Our interpretation of the nature of configuration **II** is further corroborated by the fact that Cl-up and DeCl-up are expected to orient the same way on the surface, driven by highly favorable registry of the isoindole N atoms and Cu atoms on the surface. This is indeed found to be the case both computationally and in the experimental data (see Table S1 and Figure S3 in SI).

The observation of dechlorinated molecules together with intact Cl-up molecules indicates that dechlorination is kinetically hindered. Though a detailed investigation of the mechanism for this reaction is beyond the scope of the present report, we suggest that this process is determined by the approach of the ClB-SubPc molecules toward the surface upon adsorption: When the molecule approaches with the B−Cl bond pointing away from the surface, an intact Cl-up configuration will result. Other relative orientations will lead to initial full or partial coordination of the Cl-group with the surface followed by dechlorination. In passing, we note that we found no evidence for dechlorination prior to adsorption. Rather, large crystals grow during purification, a clear indication of high molecular purity. Further, we observed an essentially constant ratio of DeCl/Cl-up molecules even after many molecular adsorption cycles from the same crucible. This indicates that the ClB-SubPc molecules remain intact during the deposition process, consistent also with a bond-breaking enthalpy of 5.6 eV for the B−Cl bond in the gas phase.[23]

Comparing these findings to literature, we note that a number of nonplanar phthalocyanines and in particular axially substituted chloro-(sub)phthalocyanines have been investigated by STM on a range of surfaces already.[23−27] In many of these systems, adsorbate configurations resembling our type **I**, that is, with a bright center, are found. These are indeed typically interpreted as Cl-up, which is in agreement with our findings. In some STM studies,[6,13,19,22,26,46] adsorbates that resemble our type **II**, that is, configurations that lack the enhanced apparent height along the central symmetry axis, are also reported. They are commonly interpreted as resulting from a configuration akin to the Cl-down situation in our work. In some instances, such an interpretation has also been developed based on photoelectron spectroscopy[23,26,47] and X-ray standing wave data.[20] In passing, we note that for the system studied in[20] dechlorination has, in fact, recently been discussed as a possible scenario.[51]

The possibility that Cl-down adsorbates are in fact the result of dechlorination on the surface has been mostly disregarded. When discussed at all, the following arguments against dechlorination are commonly made:

(i) There is no direct evidence of dechlorination of (sub)phthalocyanines on surfaces of coinage metals, such as the formation of Cl adatom clusters on the surface. Even small quantities of chlorine are known to form clusters on Cu(111) at room temperature that form incommensurate hexagonal structures.[48] Such adatom clusters are absent also in our STM pictures. This could, however, be a consequence of the aggregation of Cl atoms at defects and steps on Cu(111), which would make their direct observation difficult.

(ii) Cl adatoms on Cu(111) increase the work function even at rather small coverages,[43,49] in direct conflict with photoemission spectroscopy results for the present system.[26] For example, for ClB-SubPc on Cu(111) a work function decrease in excess of 800 meV was reported at 1 MLE.[26] This is however not necessarily conclusive evidence against dechlorination because photoemission is an area-averaged measurement, where the net change in the work function may easily be dominated by the organic adsorbate even in the presence of significant amounts of chlorine adatoms. The latter would be particularly true for the case of Fermi-level pinning, where the electron affinity of the organic adsorbate layer determines the work function.[50] We have recently observed for gallium chloride phthalocyanine on Cu(111) that the work function upon declorination is indeed determined by the energetics of the pinned phthalocyanine orbital.[51]

(iii) Dechlorination is considered to be a thermodynamically costly process requiring 5.6 eV in the gas phase,[23] making it unlikely to occur. The above number is, however, based on gas phase calculations and thus fails to acknowledge the important role of the surface. It is in fact known that the axial boron-chloride bond is labile already in the presence of moderate nucleophiles in solution.[52] Also, dechlorination is a known process for instance in the case of iron octaethylporphyrin chloride (FeCl-OEP) on Cu(111)[45] and Au(III)-tetraphenyl-porphyrin chloride ($[Au^{III}TPP]^+Cl^-$) on Au (111).[44] Note that at least in the case of FeCl-OEP on Cu(111) chlorine adatoms were not clearly visible either.

The impact of the surroundings on the dechlorination process was recently reported by Guilleme et al.,[53] who investigated the kinetics of dechlorination and hydrolysis of ClB-SubPc in solution. They observed an elevated rate of dechlorination when the solvent stabilizes partial charges formed during the reaction, further accelerated by increasing the strength of electron-donating groups substituted at the periphery of the SubPc heterocycle. Although solvents are quite different from surfaces, we propose that the dechlorination of the ClB-SubPc molecule is mediated in a somewhat similar fashion by the Cu(111) surface, which can readily stabilize partial charges and act as an electron donating pool. Guilleme et al. proposed that dechlorination involves significant stretching and deviation of the B−Cl bond away from the molecular symmetry axis. This is similar to the putative precursor to dechlorination apparent in our computational treatment: In the fallen configurations, the B−Cl bond is at least 1.94 Å long (compared to 1.84 Å in the gas phase) and deviates by 7.3° form the gas phase symmetry axis.

3.5. Growth of Adsorbate Type II: DeCl-up. In striking contrast to type **I** molecules, molecules of adsorbate type **II** do not form monolayer hcp islands readily; instead, they are generally found in isolation (Figure 7). We interpret this fundamentally different thin film formation behavior as a direct consequence of their different chemical nature. The energetic cost for rotation by 60° is small enough (see Figure 5) such that type **II** molecules are occasionally also found at the edges of Cl-up islands, reminiscent of stacking faults on crystal surfaces.

At higher coverages, DeCl-up molecules do start to form aggregates that in some cases become part of ordered structures (green circles in Figure 4). The latter have a noticeably greater apparent height than monolayer islands. A close-up of such an ordered structure is shown in Figure 8 and reveals that they consist principally of two separate components of different heights: (i) A wetting layer of molecules residing directly on the Cu(111) surface (see red dashed line in Figure 8a, connecting

DOI: 10.1021/acs.jpcc.5b11799
J. Phys. Chem. C 2016, 120, 7113−7121

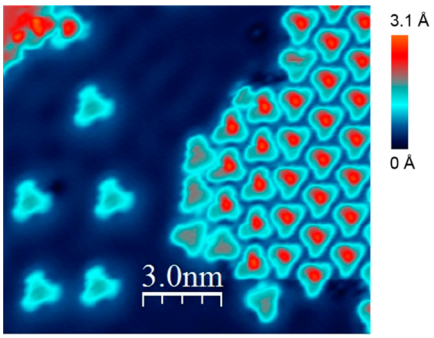

Figure 7. STM image of 0.14 MLE ClB-SubPc on Cu(111) for a film prepared at 223 K (V_S = 0.1 V; I_t = 50 pA, 5 K), contrasting film growth for Cl-up/type **I** molecules and DeCl-up/type **II** molecules.

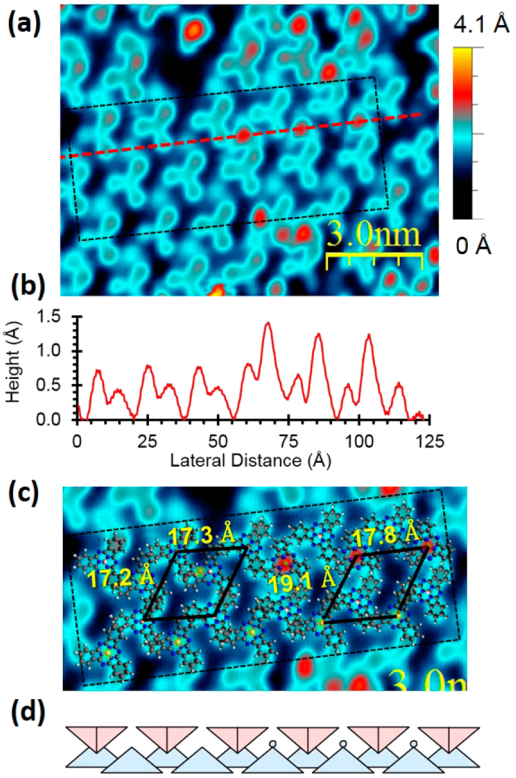

Figure 8. (a) STM image of 0.50 MLE ClB-SubPc on Cu(111) for a film prepared at 205 K (V_S = −2 V; I_t = 50 pA, 5 K) showing the bilayer structure in detail. (b) Profile of height difference along dashed red line in part (a). (c) Unit cells of wetting layer DeCl-up and second layer Cl-down molecules. (d) Side-on cartoon view of bilayer structure.

one row of these molecules); and more prominently (ii) an intercalated set of trefoil-shaped molecules with much enhanced apparent height. A small number of Cl-up molecules, identifiable by the bright central feature of the Cl-atom, are interspersed throughout the island as well (e.g., right half of red dashed line in Figure 8a), and may be considered "defects" in the island. Molecules in the wetting layer other than Cl-up defects resemble in appearance the isolated DeCl-up molecules. This assignment is further supported by comparing height changes across the island, measured along the red dashed line in Figure 8a and shown in Figure 8b. This lineout shows tall features that correspond to the Cl atom in the Cl-up molecules (height difference >1 Å), medium height features that correspond to one wing of the intercalated trefoil molecules (height difference ∼0.7 Å) and a low feature (height difference below 0.5 Å) corresponding to the center of the molecules that primarily form the wetting layer. Comparing the general appearance of the STM images in Figure 8 with the simulations from Figures 3 and 6 and considering the differences in apparent height, a wetting layer of largely DeCl-up is most consistent with the experimental data. Interspersed in this wetting layer is also a limited number of intact Cl-up molecules. An alternative assignment associating the bright protrusions between the trefoil-shaped molecules with Cl atoms which would originate from dechlorination of ClB-SubPc molecules appears unlikely, since these atoms would exhibit a significantly lower apparent height.

The trefoil molecules intercalated between lattice sites of the wetting layer are different from all other observed molecules adsorbed directly on the Cu(111) surface. They strongly resemble the simulated DeCl-down molecules shown in Figure 6a, or possibly the Cl-down molecules shown in Figure 3b. The structure of these islands is therefore interpreted as a bilayer composed of a wetting layer of DeCl-up molecules (interspersed with Cl-up defects) and an intercalated second layer of either DeCl-down or Cl-down molecules. This suggests that formation of DeCl-up islands may require stabilization by a second layer. The wetting layer of DeCl-up molecules is not packed as densely in this bilayer structure as the hcp Cl-up islands (cf. Figures 8c and 4a). The molecular arrangement is overlaid in Figure 8c and a side-on cartoon view is shown in Figure 8d. Similar bilayer structures have also been reported for iron(II) phthalocyanine on Cu(111)[54] and vanadyl phthalocyanine on Cu(111),[22] and Trelka et al. observed a similar structure for the ClB-SubPc/Cu(111) interface.[27]

4. CONCLUSION

We investigated the adsorbate structure and self-assembly at submonolayer coverages of ClB-SubPc on Cu(111) for a range of temperatures and coverages by LT-STM and density functional theory calculations. Although similar shuttle-cock shaped polar molecules have been reported to adsorb either with the polar group pointing toward or away from the surface, we find that this is not the case for ClB-SubPc on Cu(111). Instead, we observe both computationally and by STM that these molecules adsorb either as Cl-up with the Cl-atom pointing toward the vacuum side of the interface or they dechlorinate. The latter we ascribe to a reaction catalyzed at the surface even at low temperatures, which yields dechlorinated DeCl-up molecules. Both species adsorb preferentially at hcp hollow sites where maximum interaction between the N atoms of the SubPc ligand and the Cu atoms in the first surface layer is obtained. The Cl-up molecules self-assemble on the surface to form two different types of hcp islands, while the DeCl-up molecules remain isolated unless stabilized in a bilayer structure with Cl-down or DeCl-down molecules. Our results highlight that caution must be used when interpreting STM contrast for complex interfaces.

Dissociation of halogenated polar groups in molecules belonging to the phthalocyanine class may be more general, requiring a full atomistic understanding of molecular adsorption at the surface. As a consequence, the use of halogen-based dipolar groups to tailor the interfacial electronic structure is not necessarily as straightforward as typically assumed, at least not on some coinage metal surfaces. Consequently, other

DOI: 10.1021/acs.jpcc.5b11799
J. Phys. Chem. C 2016, 120, 7113−7121

approaches for a controlled work-function tuning have to be sought.

■ ASSOCIATED CONTENT

Supporting Information

The Supporting Information is available free of charge on the ACS Publications website at DOI: 10.1021/acs.jpcc.5b11799.

Atomically resolved STM images, computational results for the site-dependent adsorption energy of "DeCl-up" as well as a discussion on the inversion from "DeCl-up" to "DeCl-down" are available(PDF).

■ AUTHOR INFORMATION

Corresponding Authors

*E-mail: egbert.zojer@tugraz.at.

*E-mail: monti@u.arizona.edu. Tel: ++1 520 626 1177. Fax: ++1 520 621 8407.

Author Contributions

#N.I. and S.S.H. contributed equally to this work.

Notes

The authors declare no competing financial interest.

■ ACKNOWLEDGMENTS

The authors thank Leonhard Grill (University of Graz), Elisabeth Wruss, and Elisabeth Verwüster (TU Graz) for stimulating discussions. This research was supported by the National Science Foundation under Grant CHE-1213243 (Arizona), by the European Union Seventh Framework Programme under grant agreement n° 607232 [THINFACE] and by the Austrian Science Fund (FWF), P24666-N20. This research also used resources of the Center for Functional Nanomaterials, which is a U.S. DOE Office of Science Facility, at Brookhaven National Laboratory under Contract No. DE-SC0012704. The computational results presented have been achieved using the Vienna Scientific Cluster (VSC). We would also like to thank Dr. Björn Lange and Prof. Volker Blum at Duke University for making their new implementation of STM simulations in FHI-aims available to us.

■ REFERENCES

(1) Sykes, E. C. H.; Mantooth, B. A.; Han, P.; Donhauser, Z. J.; Weiss, P. S. Substrate-Mediated Intermolecular Interactions: A Quantitative Single Molecule Analysis. *J. Am. Chem. Soc.* **2005**, *127*, 7255−60.

(2) Eremtchenko, M.; Schaefer, J. A.; Tautz, F. S. Understanding and Tuning the Epitaxy of Large Aromatic Adsorbates by Molecular Design. *Nature* **2003**, *425*, 602−605.

(3) Chang, S.-H.; Kuck, S.; Brede, J.; Lichtenstein, L.; Hoffmann, G.; Wiesendanger, R. Symmetry Reduction of Metal Phthalocyanines on Metals. *Phys. Rev. B: Condens. Matter Mater. Phys.* **2008**, *78*, 233409.

(4) Li, Z.; Li, B.; Yang, J.; Hou, J. G. Single-Molecule Chemistry of Metal Phthalocyanine on Noble Metal Surfaces. *Acc. Chem. Res.* **2010**, *43*, 954−962.

(5) Wei, Y.; Robey, S. W.; Reutt-Robey, J. E. Flux-Selected Titanyl Phthalocyanine Monolayer Architecture on Ag (111). *J. Phys. Chem. C* **2008**, *112*, 18537−18542.

(6) Huang, Y. L.; Chen, W.; Bussolotti, F.; Niu, T. C.; Wee, A. T. S.; Ueno, N.; Kera, S. Impact of Molecule-Dipole Orientation on Energy Level Alignment at the Submolecular Scale. *Phys. Rev. B: Condens. Matter Mater. Phys.* **2013**, *87*, 085205.

(7) Fernandez-Torrente, I.; Monturet, S.; Franke, K. J.; Fraxedas, J.; Lorente, N.; Pascual, J. I. Long-Range Repulsive Interaction between Molecules on a Metal Surface Induced by Charge Transfer. *Phys. Rev. Lett.* **2007**, *99*, 176103.

(8) Schöll, A.; Kilian, L.; Zou, Y.; Ziroff, J.; Hame, S.; Reinert, F.; Umbach, E.; Fink, R. H. Disordering of an Organic Overlayer on a Metal Surface Upon Cooling. *Science* **2010**, *329*, 303−305.

(9) Barth, J. V. Molecular Architectonic on Metal Surfaces. *Annu. Rev. Phys. Chem.* **2007**, *58*, 375−407.

(10) Müller, K.; Kara, A.; Kim, T. K.; Bertschinger, R.; Scheybal, A.; Osterwalder, J.; Jung, T. A. Multimorphism in Molecular Monolayers: Pentacene on Cu(110). *Phys. Rev. B: Condens. Matter Mater. Phys.* **2009**, *79*, 245421.

(11) Stadler, C.; Hansen, S.; Kroger, I.; Kumpf, C.; Umbach, E. Tuning Intermolecular Interaction in Long-Range-Ordered Submonolayer Organic Films. *Nat. Phys.* **2009**, *5*, 153−158.

(12) Toader, M.; Shukrynau, P.; Knupfer, M.; Zahn, D. R. T.; Hietschold, M. Site-Dependent Donation/Backdonation Charge Transfer at the CoPc/Ag(111) Interface. *Langmuir* **2012**, *28*, 13325−13330.

(13) Wang, Y.; Kröger, J.; Berndt, R.; Hofer, W. Structural and Electronic Properties of Ultrathin Tin-Phthalocyanine Films on Ag(111) at the Single-Molecule Level. *Angew. Chem., Int. Ed.* **2009**, *48*, 1261−1265.

(14) Steele, M. P.; Kelly, L. L.; Ilyas, N.; Monti, O. L. A. Resonance and Localization Effects at a Dipolar Organic Semiconductor Interface. *J. Chem. Phys.* **2011**, *135*, 124702.

(15) Steele, M. P.; Blumenfeld, M. L.; Monti, O. L. A. Image States at the Interface of a Dipolar Organic Semiconductor. *J. Chem. Phys.* **2010**, *133*, 124701.

(16) Blumenfeld, M. L.; Steele, M. P.; Ilyas, N.; Monti, O. L. A. Interfacial Electronic Structure of Vanadyl Naphthalocyanine on Highly Oriented Pyrolytic Graphite. *Surf. Sci.* **2010**, *604*, 1649−1657.

(17) Adler, H.; Paszkiewicz, M.; Uihlein, J.; Polek, M.; Ovsyannikov, R.; Basova, T. V.; Chassé, T.; Peisert, H. Interface Properties of VOPc on Ni(111) and Graphene/Ni(111): Orientation-Dependent Charge Transfer. *J. Phys. Chem. C* **2015**, *119*, 8755−8762.

(18) Niu, T.; Zhou, M.; Zhang, J.; Feng, Y.; Chen, W. Dipole Orientation Dependent Symmetry Reduction of Chloroaluminum Phthalocyanine on Cu(111). *J. Phys. Chem. C* **2013**, *117*, 1013−1019.

(19) Lackinger, M.; Hietschold, M. Determining Adsorption Geometry of Individual Tin−Phthalocyanine Molecules on Ag(111)−−a STM Study at Submonolayer Coverage. *Surf. Sci.* **2002**, *520*, L619−L624.

(20) Gerlach, A.; Hosokai, T.; Duhm, S.; Kera, S.; Hofmann, O. T.; Zojer, E.; Zegenhagen, J.; Schreiber, F. Orientational Ordering of Nonplanar Phthalocyanines on Cu(111): Strength and Orientation of the Electric Dipole Moment. *Phys. Rev. Lett.* **2011**, *106*, 156102.

(21) Yamane, H.; Honda, H.; Fukagawa, H.; Ohyama, M.; Hinuma, Y.; Kera, S.; Okudaira, K. K.; Ueno, N. HOMO-Band Fine Structure of OTi- and Pb-Phthalocyanine Ultrathin Films: Effects of the Electric Dipole Layer. *J. Electron Spectrosc. Relat. Phenom.* **2004**, *137*−*140*, 223−227.

(22) Niu, T.; Zhang, J.; Chen, W. Molecular Ordering and Dipole Alignment of Vanadyl Phthalocyanine Monolayer on Metals: The Effects of Interfacial Interactions. *J. Phys. Chem. C* **2014**, *118*, 4151−4159.

(23) Berner, S.; de Wild, M.; Ramoino, L.; Ivan, S.; Baratoff, A.; Güntherodt, H.-J.; Suzuki, H.; Schlettwein, D.; Jung, T. A. Adsorption and Two-Dimensional Phases of a Large Polar Molecule: Subphthalocyanine on Ag(111). *Phys. Rev. B: Condens. Matter Mater. Phys.* **2003**, *68*, 115410.

(24) Jiang, N.; Wang, Y.; Liu, Q.; Zhang, Y.; Deng, Z.; Ernst, K.-H.; Gao, H.-J. Polymorphism and Chiral Expression in Two-Dimensional Subphthalocyanine Crystals on Au(111). *Phys. Chem. Chem. Phys.* **2010**, *12*, 1318−1322.

(25) Mannsfeld, S.; Reichhard, H.; Fritz, T. LEED and STM Investigation of Chloro(subphthalocyaninato)boron on Au(111). *Surf. Sci.* **2003**, *525*, 215−221.

(26) Ilyas, N.; Monti, O. L. A. Interplay of Local and Global Interfacial Electronic Structure of a Strongly Coupled Dipolar Organic Semiconductor. *Phys. Rev. B: Condens. Matter Mater. Phys.* **2014**, *90*, 125435.

(27) Trelka, M.; Medina, A.; Écija, D.; Urban, C.; Gröning, O.; Fasel, R.; Gallego, J. M.; Claessens, C. G.; Otero, R.; Torres, T.; Miranda, R. Subphthalocyanine-Based Nanocrystals. *Chem. Commun.* **2011**, *47*, 9986.
(28) Zahl, P.; Wagner, T.; Möller, R.; Klust, A. Open Source Scanning Probe Microscopy Control Software Package GXSM. *J. Vac. Sci. Technol. B Microelectron. Nanometer Struct.* **2010**, *28*, C4E39.
(29) Zahl, P.; Bierkandt, M.; Schröder, S.; Klust, A. The Flexible and Modern Open Source Scanning Probe Microscopy Software Package GXSM. *Rev. Sci. Instrum.* **2003**, *74*, 1222.
(30) Horcas, I.; Fernández, R.; Gómez-Rodríguez, J. M.; Colchero, J.; Gómez-Herrero, J.; Baro, A. M. WSXM: a Software for Scanning Probe Microscopy and a Tool for Nanotechnology. *Rev. Sci. Instrum.* **2007**, *78*, 013705.
(31) Blum, V.; Gehrke, R.; Hanke, F.; Havu, P.; Havu, V.; Ren, X.; Reuter, K.; Scheffler, M. Ab initio Molecular Simulations with Numeric Atom-Centered Orbitals. *Comput. Phys. Commun.* **2009**, *180*, 2175−2196.
(32) Perdew, J. P.; Burke, K.; Ernzerhof, M. Generalized Gradient Approximation Made Simple. *Phys. Rev. Lett.* **1996**, *77*, 3865−3868.
(33) Tkatchenko, A.; Scheffler, M. Accurate Molecular Van Der Waals Interactions from Ground-State Electron Density and Free-Atom Reference Data. *Phys. Rev. Lett.* **2009**, *102*, 073005.
(34) Ruiz, V. G.; Liu, W.; Zojer, E.; Scheffler, M.; Tkatchenko, A. Density-Functional Theory with Screened van der Waals Interactions for the Modeling of Hybrid Inorganic-Organic Systems. *Phys. Rev. Lett.* **2012**, *108*, 146103.
(35) Liu, W.; Tkatchenko, A.; Scheffler, M. Modeling Adsorption and Reactions of Organic Molecules at Metal Surfaces. *Acc. Chem. Res.* **2014**, *47*, 3369−3377.
(36) Hofmann, O. T.; Atalla, V.; Moll, N.; Rinke, P.; Scheffler, M. Interface Dipoles of Organic Molecules on Ag(111) in Hybrid Density-Functional Theory. *New J. Phys.* **2013**, *15*, 123028.
(37) Neugebauer, J.; Scheffler, M.; Adsorbate-Substrate. and Adsorbate-Adsorbate Interactions of Na and K Adlayers on Al(111). *Phys. Rev. B: Condens. Matter Mater. Phys.* **1992**, *46*, 16067−16080.
(38) Monkhorst, H. J.; Pack, J. D. Special Points for Brillouin-Zone Integrations. *Phys. Rev. B* **1976**, *13*, 5188−5192.
(39) Tersoff, J.; Hamann, D. R. Theory of the Scanning Tunneling Microscope. *Phys. Rev. B: Condens. Matter Mater. Phys.* **1985**, *31*, 805−813.
(40) Heimel, G.; Romaner, L.; Brédas, J.-L.; Zojer, E. Organic/Metal Interfaces in Self-Assembled Monolayers of Conjugated Thiols: A First-Principles Benchmark Study. *Surf. Sci.* **2006**, *600*, 4548−4562.
(41) Stukowski, A. Visualization and Analysis of Atomistic Simulation Data with OVITO−the Open Visualization Tool. *Modell. Simul. Mater. Sci. Eng.* **2010**, *18*, 015012.
(42) Willenbockel, M.; Maurer, R. J.; Bronner, C.; Schulze, M.; Stadtmüller, B.; Soubatch, S.; Tegeder, P.; Reuter, K.; Tautz, F. S. Coverage-Driven Dissociation of Azobenzene on Cu(111): a Route Towards Defined Surface Functionalization. *Chem. Commun.* **2015**, *51*, 15324−15327.
(43) Peljhan, S.; Kokalj, A. Adsorption of Chlorine on Cu(111): A Density-Functional Theory Study. *J. Phys. Chem. C* **2009**, *113*, 14363−14376.
(44) Heinrich, B. W.; Ahmadi, G.; Müller, V. L.; Braun, L.; Pascual, J. I.; Franke, K. J. Change of the Magnetic Coupling of a Metal−Organic Complex with the Substrate by a Stepwise Ligand Reaction. *Nano Lett.* **2013**, *13*, 4840−4843.
(45) van Vörden, D.; Lange, M.; Schaffert, J.; Cottin, M. C.; Schmuck, M.; Robles, R.; Wende, H.; Bobisch, C. A.; Möller, R. Surface-Induced Dechlorination of FeOEP-Cl on Cu(111). *ChemPhysChem* **2013**, *14*, 3472−3475.
(46) Niu, T.; Zhou, C.; Zhang, J.; Zhong, S.; Cheng, H.; Chen, W. Substrate Reconstruction Mediated Unidirectionally Aligned Molecular Dipole Dot Arrays. *J. Phys. Chem. C* **2012**, *116*, 11565−11569.
(47) Blumenfeld, M. L.; Steele, M. P.; Monti, O. L. A. Near- and Far-Field Effects on Molecular Energy Level Alignment at an Organic/Electrode Interface. *J. Phys. Chem. Lett.* **2010**, *1*, 145−148.
(48) Andryushechkin, B. V.; Eltsov, K. N.; Shevlyuga, V. M. Domain-Wall Mechanism of "$(n\sqrt{3} \times n\sqrt{3})R30°$" Incommensurate Structure Formation in Chemisorbed Halogen Layers on Cu(111). *Surf. Sci.* **2000**, *470*, L63−L68.
(49) Roman, T.; Groß, A. Periodic Density-Functional Calculations on Work-Function Change Induced by Adsorption of Halogens on Cu(111). *Phys. Rev. Lett.* **2013**, *110*, 156804.
(50) Hofmann, O. T.; Egger, D. A.; Zojer, E. Work-Function Modification beyond Pinning: When Do Molecular Dipoles Count? *Nano Lett.* **2010**, *10*, 4369−4374.
(51) Wruss, E.; Hofmann, O. T.; Egger, D. A.; Verwüster, E.; Gerlach, A.; Schreiber, F.; Zojer, E. On the Adsorption Behavior of Nonplanar Phthalocyanines. *J. Phys. Chem. C* **2016**, DOI: 10.1021/acs.jpcc.6b00312.
(52) Potz, R.; Goldner, M.; Huckstadt, H.; Cornelissen, U.; Tutass, A.; Homborg, H. Synthesis and Structural Characterization of Boron Subphthalocyaninates. *Z. Anorg. Allg. Chem.* **2000**, *626*, 588−596.
(53) Guilleme, J.; Martínez-Fernández, L.; González-Rodríguez, D.; Corral, I.; Yáñez, M.; Torres, T. An Insight into the Mechanism of the Axial Ligand Exchange Reaction in Boron Subphthalocyanine Macrocycles. *J. Am. Chem. Soc.* **2014**, *136*, 14289−14298.
(54) Scarfato, A.; Chang, S.-H.; Kuck, S.; Brede, J.; Hoffmann, G.; Wiesendanger, R. Scanning Tunneling Microscope Study of Iron(II) Phthalocyanine Growth on Metals and Insulating Surfaces. *Surf. Sci.* **2008**, *602*, 677−683.

DOI: 10.1021/acs.jpcc.5b11799
J. Phys. Chem. C 2016, 120, 7113−7121